Supplementary information

1. Signal selection with TSXRD

A SXRD measurement of a polycrystalline surface, even with a narrow beam, contain diffraction from multiple grains due to the long X-ray beam footprint, caused by the grazing incidence angle needed to distinguish the weak surface signals. This is shown as an example in Fig. S1, recorded from the polycrystalline Au electrode discussed in the main text, where a single rotation shows partial diffraction patterns from multiple grains. A movie showing a 180° rotation is included as SI.

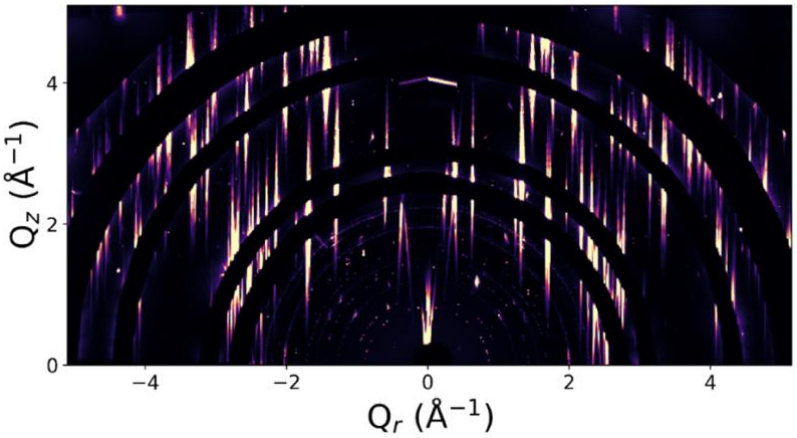

Figure S1: An example of a single rotation at the centre of the sample. Here, $Q_r = \sqrt{Q_x^2 + Q_y^2}$. Since different grains are measured at different angles, this is a combination of partial diffraction patterns of different grains.

In the sorting procedure (Fig. S2), the grain map from tomographic grazing incidence X-ray (TGIXRD) is reduced to a projection of each grain at each angle of the sample rotation. This will give an extension of the grain perpendicular to the beam (Δy). The length of the grain along the beam direction (x) can be calculated for each Δy.

From the repetitive measurement procedure described in the methodology, all parts of the sample surface are measured at a large angular range. From each image at a certain angle, a diffraction signal can be studied for all Δy. The signal should only be present at the Δy where its grain of origin is measured. Thus, the intensity of the CTR for each Δy can be compared to the projection of the grains at this angle, to assign the signal to a grain. At the thinner parts of the grains, where the path over the sample is shorter, and at the boundaries, the signal is sometimes missing, either due to low intensity from the short path over the grain, or due to uncertainties in the boundaries of the grain map. To further confirm the assignment of CTRs, they can be compared to the Bragg spots from the TGIXRD mapping of the grain as in Fig. 9b.

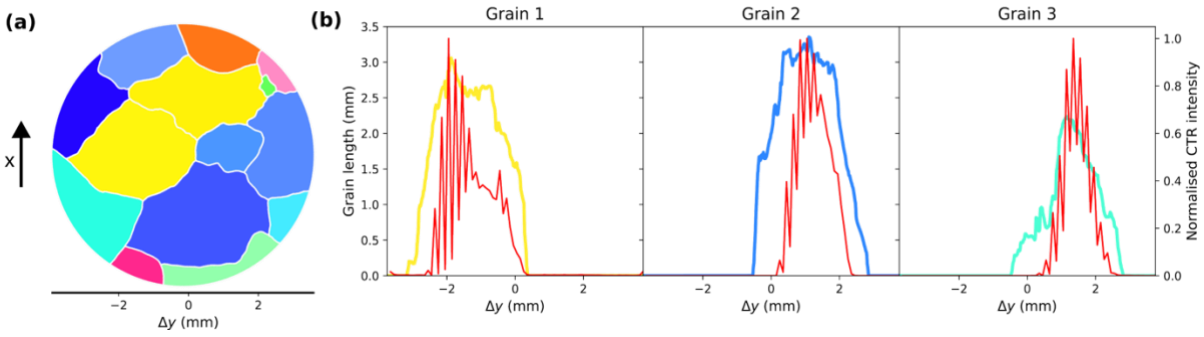

Figure S2: a) The map rotated to the central angle of the fast measurement of grain 1. The grain projection can be achieved by taking the length of the grain along x for each Δy. b) The projections of the grains to the Δy-axis (coloured). The CTR intensity, normalised to the maximum intensity, in all images at different Δy for the central angle of the measurements of the grains. The comparison of the projection to the signal confirms a correct assignment.

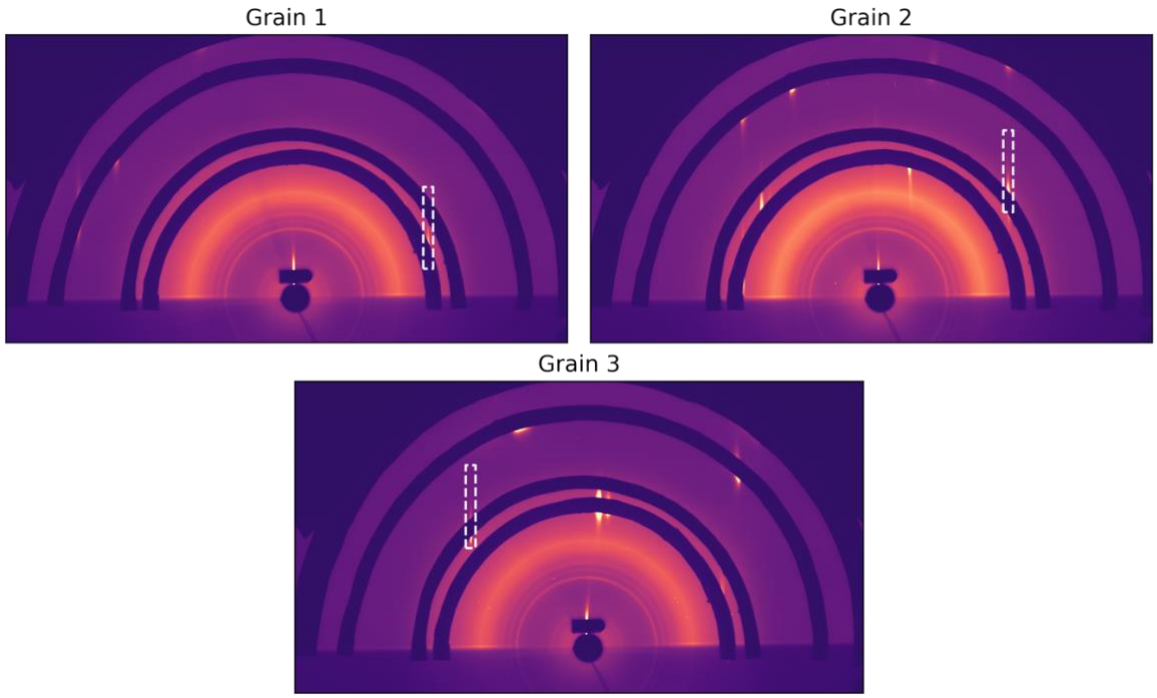

Figure S3: The diffraction image from the 4° scan for each grain shown as the maximum intensity registered for each pixel. The white box defines the magnified area around the CTR of interest shown in Fig. 9b.

2. Scanning TSXRD

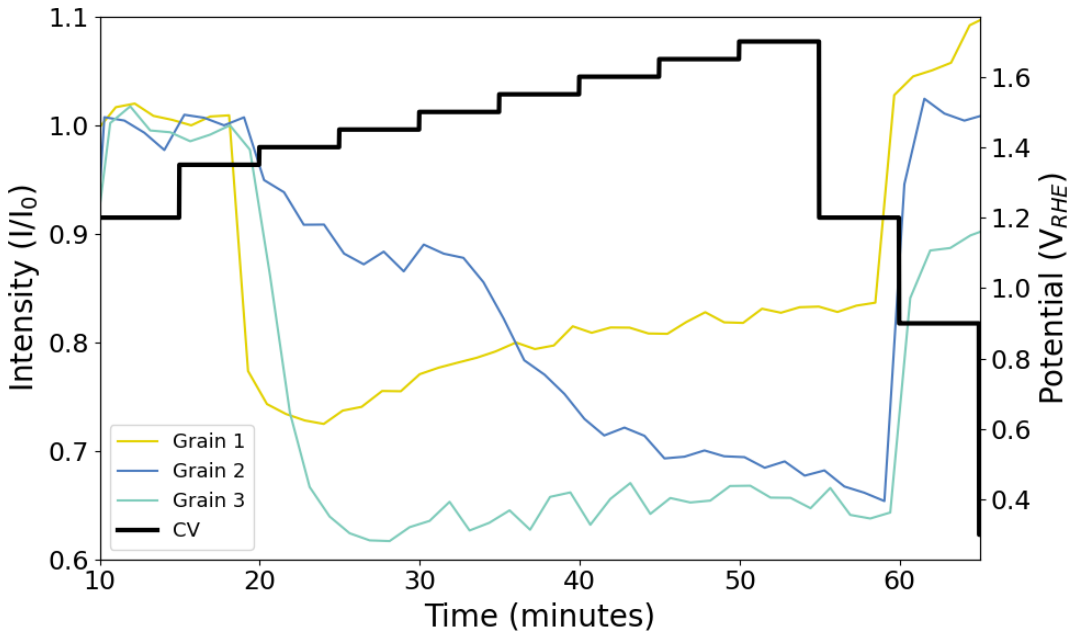

Figure S4: Scanning SXRD of the three grains of interest during potential steps. The intensity is normalised to a point at the plateau before the onset to highlight the difference in oxidation onset time. Since the time at each potential is relatively long, the system has more time to react. The early oxidation of grain 1 can be observed and the two-step oxidation of grain 2 is also clearly visible.

3. Determination of oxide thickness from change in normalised SOR intensity

The change in normalised intensity R/R_0 can be related to the oxide thickness using the Fresnel's equation,[1] as shown in Eq. S1, where the Fresnel coefficients r_{ij} is defined in Eq. S2, and change in phase β is defined in Eq. S3.

$$R = \left| \frac{r_{12} + r_{23}e^{i2\beta}}{1 + r_{12}r_{23}e^{i2\beta}} \right|^2 \quad (S1)$$

$$r_{ij} = \frac{n_i - n_j}{n_i + n_j} \quad (S2)$$

$$\beta = \frac{2\pi n_2 d}{\lambda} \quad (S3)$$

$n_1, n_2, and\ n_3$ represent the complex refractive indices of the electrolyte, Au oxide (Au_2O_3), and Au metal, respectively. d is the thickness of the oxide, and λ is the wavelength of the light. $R_0 = 1$ is the initial intensity where $d = 0$.

The change in normalised intensity calculated as a function of the Au oxide thickness is shown in Fig. S5. The refractive indices used were $n_1 = 1.33 + i1.87^{-8}$ (value taken for pure water) [2], $n_2 = 3.3 + i1.3$ [3], and $n_3 = 0.14 + i3.7$ [4].

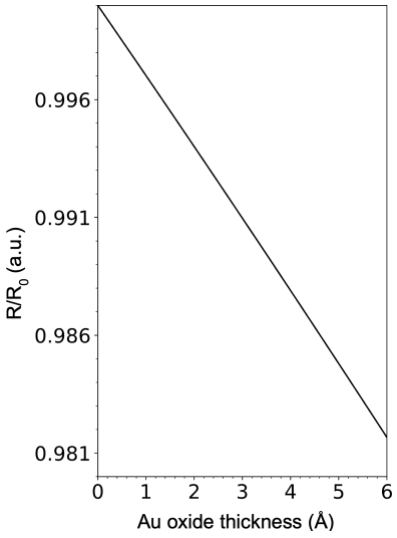

Figure S5: Normalised intensity calculated using Fresnel's equation as a function of the Au oxide thickness.

4. 2D-SOR of other grains of polycrystalline Au

Although three grains of interest were discussed in the main paper, additional grains could be spatially resolved in the 2D-SOR experiment. A total of ten grains were analysed, summarised in Fig. S6. From the EBSD measurement of the polycrystalline Au, the orientations of the grains were determined, and visualised in a grain-map, as shown in Fig. S6a. The normalised reflectance of the 10 grains as a function of time is overlaid with the CV (Fig. S6b), where similar grain orientations exhibit similar changes in reflectance across the broad Au oxidation peak. This is also reflected in the time derivative of the normalised SOR reflectance of the grains in Fig. S6c.

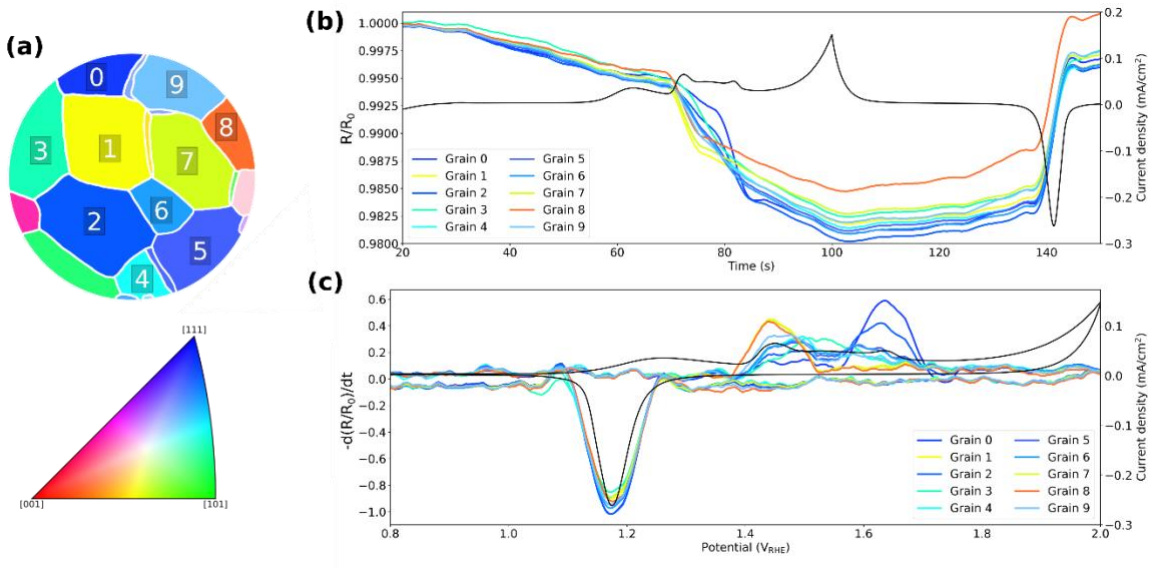

Figure S6: a) EBSD grain map of the polycrystalline Au labelled with 10 identified grains of different surface orientations. b) Normalised reflectance from SOR of the identified grains. c) Time derivative of the normalised reflectance of the identified grains.

The summation of the time derivates of the identified grains resemble the CV, as in Fig. S7a, and the difference could be attributed to other grains that were not analysed, or the sides of the sample that were exposed to EC treatment but not captured with 2D-SOR. Additionally, the oxide thicknesses of the grains were estimated, as shown in Fig. S7b.

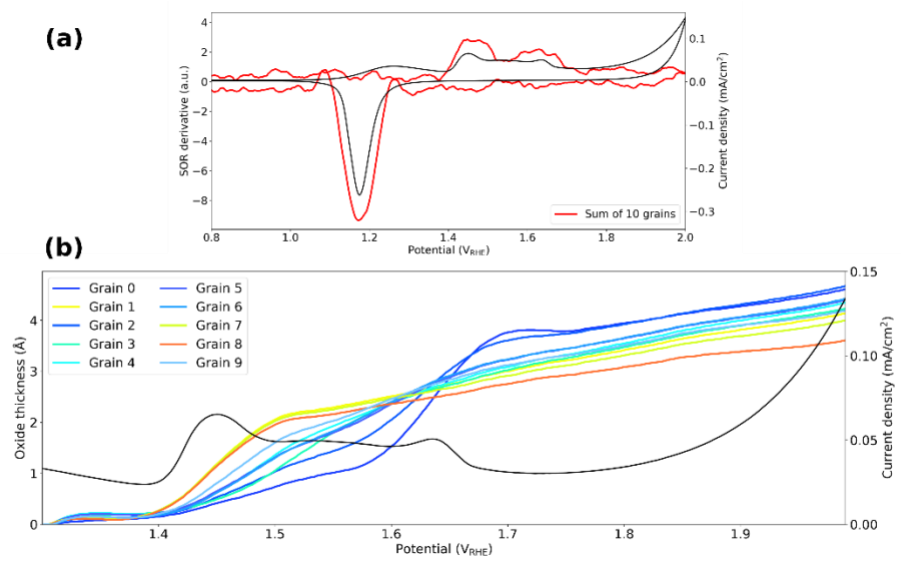

Figure S7: a) Summation of time derivatives of the 10 grains, overlaid with the CV as a function of potential. b) Oxide thickness of the 10 grains estimated using Fresnel's equation.

5. EC measurement procedure for EC-NAPXPS experiment

When the electrodes are in dip configuration, an example of the EC measurement procedure is as shown in Fig. S8. A CV cycle is performed to verify the features expected from the polycrystalline Au sample, followed by a half CV cycle (forward scan) to 1.7 V_{RHE}. Subsequently, a potential of 1.7 V_{RHE} is applied during chronoamperometry (measuring current). The sample is only pulled out of the electrolyte for XPS measurements when a steady-state current is achieved (~ 60 s in this example).

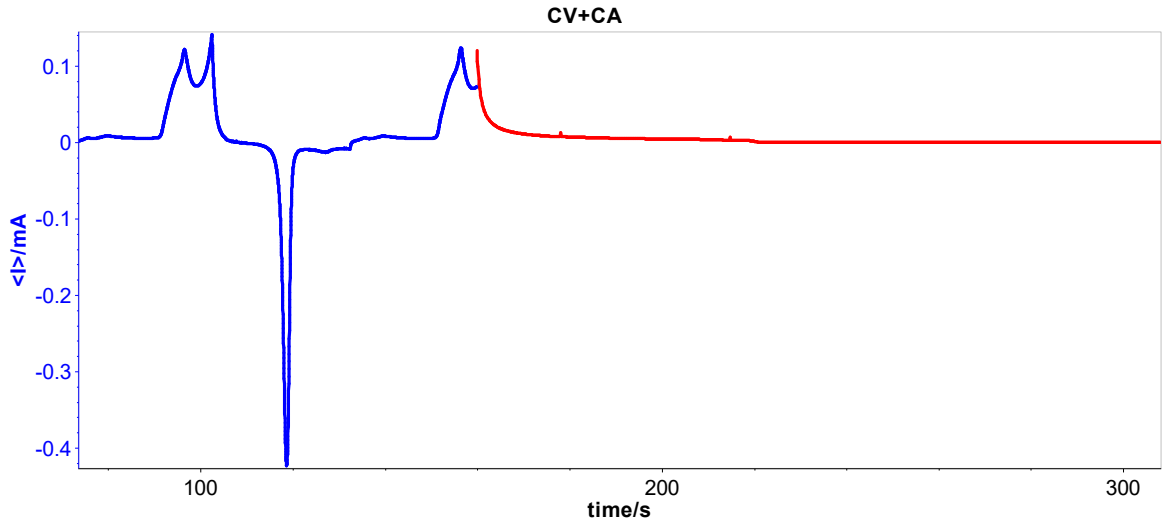

Figure S8: Example 1.5 CV cycle (blue line), and subsequent chronoamperometry measurement with applied potential of 1.7 V_{RHE} (red line).

6. EC-NAPXPS fitting parameters

The Au 4f metal and interface components were fitted with an asymmetric pseudo-Voigt profile,[5] and the Au oxide/hydroxide components were fitted with a Voigt profile from the python package LMFIT. The spectra were Shirley background subtracted before peak fitting.

Table S1: Peak fitting parameters

Chemical state	Binding energy (eV)	Gaussian width	Lorentzian width	FWHM	Gauss-Lor mixing parameter	Asymmetry parameter	Spin- orbit splitting	Spin-orbit ratio
Au $4f_{7/2}$ metal	83.9 ± 0.001	0.20	0.23	0.61	0.819	2.23	3.68	1.33
Au $4f_{7/2}$ interface	83.327 ± 0.001	0.20	0.23	0.64	0.971	2.99	3.68	1.33
Au $4f_{7/2}$ oxide/ hydroxide	85.527 ± 0.001	0.53	0.2	1.458	-	-	3.68	1.33

7. EC-NAPXPS thickness calculation

From the fitted components from the XPS spectra, the oxide/hydroxide thickness can be estimated using a simplified assumption that the metallic Au and oxide/hydroxide are modelled as continuous layers. By taking the fitted normalised area ratios between the oxide/hydroxide and metallic Au components, the oxide thicknesses can be calculated using Eq. S4,

$$d_{ox} = \lambda^{Ox} \cdot \sin\theta \cdot \ln\left[1 + \frac{N^{Au}\lambda^{Au}I^{Ox}}{N^{Ox}\lambda^{Ox}I^{Au}}\right] \quad (S4)$$

Where d is the thickness, λ is the IMFP of electrons of the different components, θ is the emission angle of the photoelectrons (normal emission: 90°), N is the atomic density of the different components, and I is the normalised area of the fitted XPS component. For the main text, the constants of metallic Au and Au oxide (Au_2O_3) were used, as tabulated in Tab. S2. The constants of Au oxyhydroxide ($HAuO_2$) are also tabulated, and the oxide thickness estimation is shown in Fig. S9. A comparison of the thickness between using Au_2O_3 and $HAuO_2$ is summarised in Tab. S3.

Table S2: Constants used for oxide thickness calculation. The IMFP values are calculated using the QUASES-TPP2M software.[6]

	Metallic Au	$HAuO_2$	Au_2O_3
Density (g/cm³)	19.32 [7]	8.26 [8]	11.34 [9]
Molar mass (g/mol)	196.97 [7]	229.97 [10]	441.93 [9]
Atomic density (mol/cm³)	0.098	0.036	0.051
IMFP (λ @ 1116 eV) (Å)	13.33	19.96	15.72

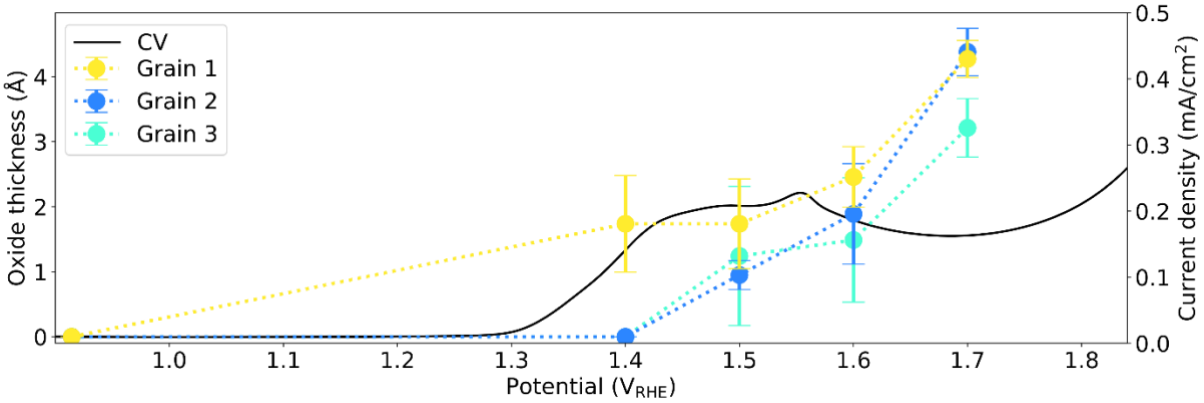

Figure S9: Oxide thickness of the Au hydroxide ($HAuO_2$) (dotted lines and solid dots with error bars), derived from the intensity ratio between the Au oxide/hydroxide and bulk Au peaks from the fitted XPS spectra as a function of potential together with the forward direction of the CV (black line). The potential range of the CV is 0.25–1.85 V_{RHE} at 50 mV/s. The black arrows indicate scan direction.

Table S3: Summary of oxide thicknesses (Å) estimated from EC-NAPXPS, assuming the Au_2O_3 or $HAuO_2$.

Oxide thickness (Å)								
Potential (V_{RHE})	1.4		1.5		1.6		1.7	
Method	Au_2O_3	$HAuO_2$	Au_2O_3	$HAuO_2$	Au_2O_3	$HAuO_2$	Au_2O_3	$HAuO_2$
Grain 1	1.2	1.7	1.2	1.7	1.7	2.5	3.0	4.3
Grain 2	0	0	0.7	1.0	1.3	1.9	3.1	4.4
Grain 3	0	0	0.9	1.2	1.1	1.5	2.3	3.2

8. EC differences between the experiments

Table S4: Differences between CV procedure and acidic H_2SO_4 electrolyte.

	2D-SOR	**EC-NAPXPS**	**TSXRD**
Scan rate (mV/s)	20	50	10
Electrolyte (M)	0.1 (pH=1)	0.05 (pH=1.3)	0.05 (pH=1.3)
Ref. electrodes	Ag/AgCl (sat'd KCl)	Ag/AgCl (sat'd KCl)	Reference Hydrogen Electrode

9. CV feature relating to H_2O_2 oxidation

The full CV as presented in Fig. 4e of the main text is shown in Fig. S10. Here, we observe cathodic current at potentials between 0.2 V_{RHE} – 0.5 V_{RHE}. This is associated to the oxygen reduction reaction, where in the presence of oxygen in the electrolyte, reduces O_2 to either H_2O or H_2O_2. The H_2O_2 in the electrolyte is then oxidised, contributing to the weaker broad feature between 1 and 1.3 V_{RHE}.

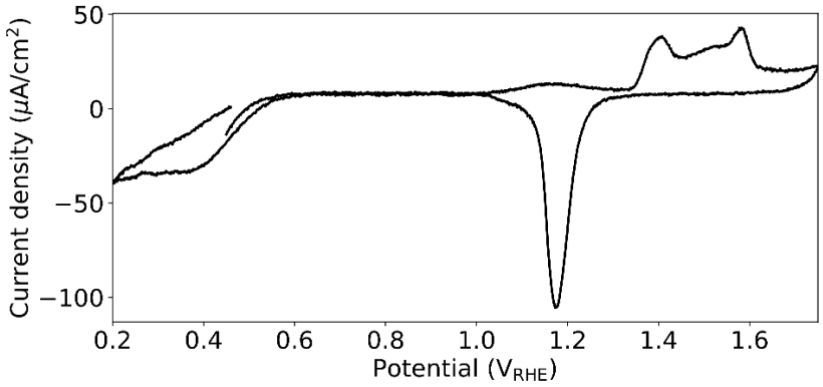

Figure S10: Full CV of potential range 0.2–1.75 V_{RHE} at 10 mV/s.

10. Oxide thickness comparison between EC-NAPXPS and 2D-SOR

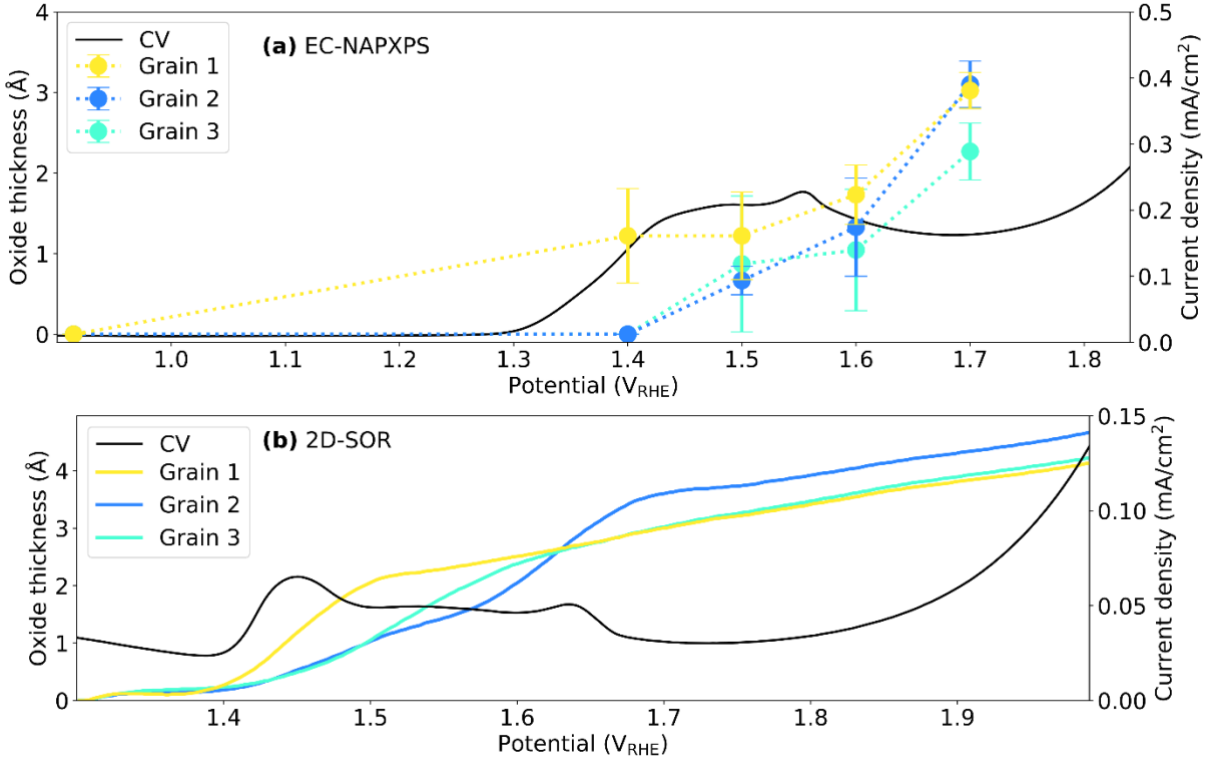

Figure S11: Comparison of oxide thickness between a) EC-NAPXPS and b) 2D-SOR. Note the difference in potential range between the experiments.

References

1. McIntyre, J. D. E. & Aspnes, D. E. Differential reflection spectroscopy of very thin surface films. *Surface Science* **24**, 417–434 (1971).
2. Hale, G. M. & Querry, M. R. Optical Constants of Water in the 200-nm to 200-µm Wavelength Region. *Appl. Opt., AO* **12**, 555–563 (1973).
3. Horkans, J., Cahan, B. D. & Yeager, E. Electrode potential scanning ellipsometric spectroscopy: Study of the formation of the anodic oxide film on noble metals. *Surface Science* **46**, 1–23 (1974).
4. Johnson, P. B. & Christy, R. W. Optical Constants of the Noble Metals. *Phys. Rev. B* **6**, 4370–4379 (1972).
5. Schmid, M., Steinrück, H. & Gottfried, J. M. A new asymmetric Pseudo-Voigt function for more efficient fitting of XPS lines. *Surface & Interface Analysis* **46**, 505–511 (2014).
6. Tanuma, S., Powell, C. J. & Penn, D. R. Calculations of electron inelastic mean free paths. V. Data for 14 organic compounds over the 50–2000 eV range. *Surface and Interface Analysis* **21**, 165–176 (1994).
7. Gold - Element information, properties and uses | Periodic Table. https://periodic-table.rsc.org/element/79/gold.
8. NIST-JARVIS. JVASP-30504_HAuO2. https://www.ctcms.nist.gov/~knc6/jsmol/JVASP-30504.html.
9. Korhonen, E. Au2O3. https://wiki.aalto.fi/display/SSC/Au2O3.
10. Hydroxy(oxo)gold. https://www.chemspider.com/Chemical-Structure.23354356.html.